13th World Conference on Earthquake Engineering
Vancouver, B.C., Canada
August 1-6, 2004
Paper No. 1643

THE ROLE OF PALEOLIQUEFACTION STUDIES IN PERFORMANCE-BASED EARTHQUAKE ENGINEERING IN THE CENTRAL-EASTERN UNITED STATES

Russell A. GREEN[1], Stephen F. OBERMEIER[2], and Scott M. OLSON[3]

SUMMARY

The implementation of performance-based earthquake engineering requires determination of both the fragility of structural systems and the probabilistic seismic hazard. In regions of low-to-moderate seismicity, such as the central and eastern United States (CEUS), the historic earthquake record is too short to determine the magnitude recurrence relationship for earthquakes larger than approximately M4.5. Thus, probabilistic quantification of the seismic hazard is greatly impeded. Paleoseismology utilizing paleoliquefaction investigations is a viable approach to extend the earthquake record to prehistoric times in the CEUS, allowing the recurrence time of moderate-to-large earthquakes to be established. However, previous interpretations of prehistoric strength of shaking using these liquefaction effects have been questionable because of the lack of having appropriate geotechnical techniques. The authors have recently developed both field and analytical techniques, outlined in Obermeier [1], Olson [2], and Green [3], which we believe should resolve these deficiencies. As a case-history example illustrating our new methods, we re-assessed the magnitude of the Vincennes earthquake that occurred in the Wabash Valley (southern Illinois/Indiana) about 6,100 years BP to be approximately M7.5. Similar assessments could be used in other relatively high seismic regions of the CEUS, such as Charleston, South Carolina and the New Madrid Seismic Zone. Our new techniques are applicable in many field settings, worldwide, irrespective of tectonic setting.

INTRODUCTION

Tremendous advances have been made in structural and geotechnical earthquake engineering, and supporting sciences, over the past several decades. However, the seismic risk to the infrastructure in the U.S. has increased, as quantified in terms of loss estimates resulting from future earthquakes. To reverse this trend, the earthquake engineering community has been moving toward performance-based earthquake engineering (PBEE), or more broadly, performance-based design (PBD). As opposed to the traditional

[1] Assistant Professor, Department of Civil and Environmental Engineering, University of Michigan, 2372 G.G. Brown Building, Ann Arbor, MI, 48109-2125, rugreen@engin.umich.edu
[2] Emeritus, U.S. Geological Survey, Reston, VA, and EqLiq Consulting, Rockport, IN, sobermei@yahoo.com
[3] Geotechnical Project Manager, URS Corporation, 1001 Highlands Plaza Drive West, Suite 300, St. Louis, MO, 63110, scott_olson@urscorp.com

design approach, wherein life safety was the primary design goal, structural design in PBEE is governed by a targeted performance level having an associated annual probability of exceedance. This concept is illustrated in Figure 1, which was adapted from 2000 Edition of the NEHRP Recommended Provisions for Seismic Regulations for New Buildings and Other Structures (NEHRP [4]). In this figure, four targeted performance levels are specified (i.e., Operational, Immediate Occupancy, Life Safe, and Near Collapse) corresponding to three levels of grounds motions (i.e., Frequent Earthquake, Design Earthquake, and Maximum Considered Earthquake). Structures are grouped into three categories (i.e., Groups I, II, and III) based on their occupancy and the relative consequences of earthquake induced damage. Structures falling into each group have specified minimum performance levels corresponding to the three levels of ground motion. Group III structures require the highest level of performance and include essential facilities required for post-earthquake recovery (e.g., hospitals and fire stations). Group II structures are those having high occupancy, such as high rise office buildings and auditoriums, and Group I structures are generally referred to as "typical" structures.

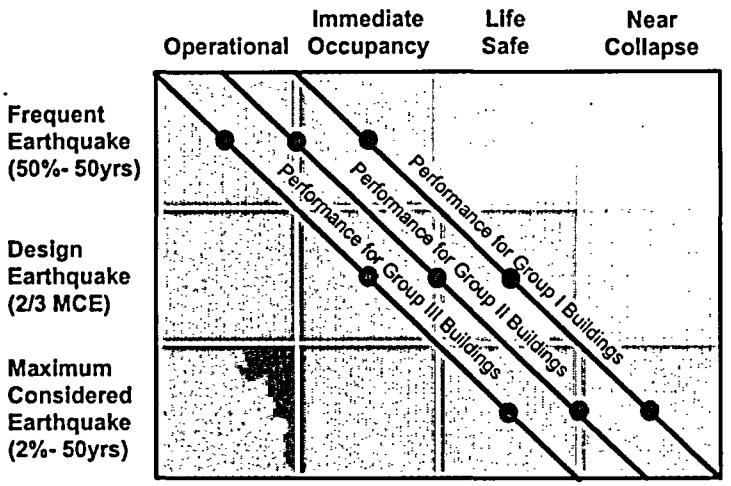

Figure 1. Building performance levels specified in the NEHRP Provisions. (Adapted from NEHRP [4])

As is readily apparent from Figure 1, proper implementation of PBEE requires knowledge of both the fragility of the structural system and the probabilistic seismic hazard. In relation to this latter requirement, the recurrence times of various magnitude earthquakes are needed for the region of interest. Magnitude recurrence is often quantified using Gutenberg-Richter type relations (or "b-line"), as illustrated in Figure 2. In this figure, the horizontal axis is earthquake magnitude, and the vertical axis is the annual number of events greater than or equal to a given magnitude. In most locations in the central and eastern U.S. (CEUS), the historical earthquake record is too short to provide information regarding the recurrence time of earthquakes above approximately M4.5, as large magnitude events occur much less frequently than smaller events. Yet, there is historical knowledge of the occurrence of moderate-to-large magnitude earthquakes (i.e., $\geq$ M 5.5) in the CEUS, such as the 1811-1812 New Madrid, Missouri, and the 1886 Charleston, South Carolina events. Consequently, geologic (or paleoseismic) investigations are being used evermore frequently to establish the recurrence time of moderate-to-large earthquakes in regions of low-to-moderate seismicity. By extending the earthquake record into prehistoric times, paleoseismology removes one of the major obstacles to implementing PBEE in the CEUS.

In this paper, we first present a brief overview of paleoseismology, with emphasis on studies performed in the CEUS. Next, we describe the major attributes and advantages of a newly proposed methodology to collect, interpret, and back-analyze paleoliquefaction field data to evaluate the prehistoric strength of

shaking (in terms of peak ground acceleration and magnitude). Finally, the authors present preliminary results using their procedures to re-evaluate the magnitude of the Vincennes earthquake that occurred in the Wabash Valley area (southern Indiana/Illinois) about 6,100 years BP.

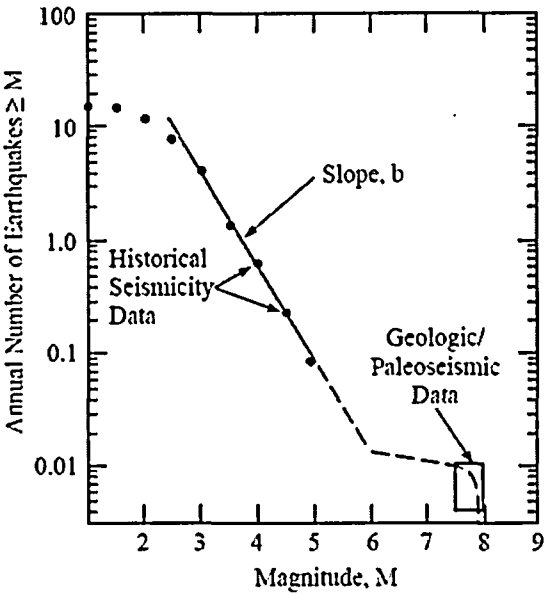

Figure 2. Gutenberg-Richter type magnitude recurrence relation (often referred to as the "b-line") used in probabilistic seismic hazard analyses. (Adapted from Schwartz [5])

OVERVIEW OF PALEOSEISMOLOGY

McCalpin [6] developed a three-tier hierarchical classification system for paleoseismic features based on the genesis, location, and timing of their manifestation. In the first tier (i.e., genesis) features are subdivided into two categories, primary and secondary, where the former result from tectonic deformations and the latter result from seismic shaking. Schematic depictions of primary and secondary paleoseismic features are shown in Figure 3. McCalpin [6] based the dimensions shown on the left side of Figure 3 on correlations developed by Wells [7].

The right side of Figure 3 shows the maximum distance from induced liquefaction (secondary evidence) to the energy center of the causative earthquake. (We use the term "energy center" as being the central region of strongest bedrock shaking.) Liquefaction is a phenomenon that occurs when the skeleton of loose, saturated sandy soil collapses and there is a temporary transfer of the overburden stress from the soil skeleton to the pore fluid. The collapse of the soil skeleton can be initiated in a variety of ways, one of which is earthquake shaking. The occurrence of liquefaction often manifests itself on the soil surface in the form of sand boils (or sand blows), as depicted in cross-sectional view in Figure 4. The authors based the distances shown in Figure 3 on a correlation developed by Ambraseys [8] for shallow crustal earthquakes worldwide. The threshold magnitude for inducing liquefaction ranges from M4.5 to M5. An estimate of the age of a paleoliquefaction feature can be made in many cases using radiocarbon dating or archeological evidence (e.g., Munson [9]; Tuttle [10]). However, exact dating of sand boils typically requires conditions where the liquefied material vented to the ground surface having organics, or requires the dikes to cross-cut a relevant buried organic-bearing stratum.

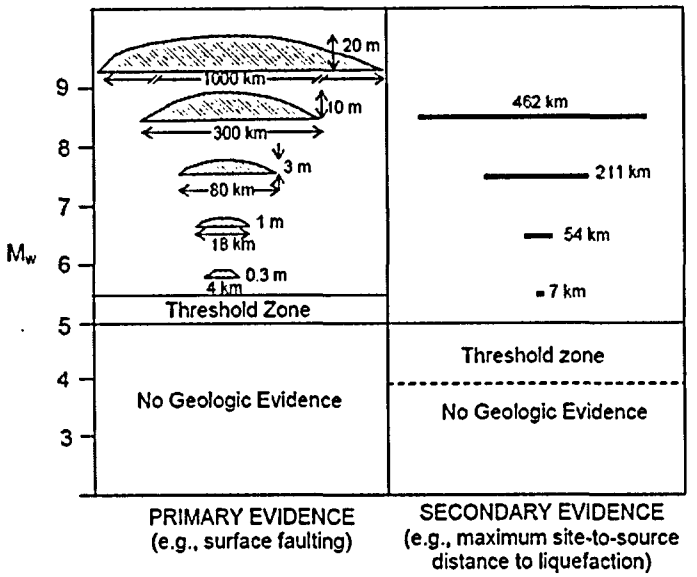

Figure 3. Schematic diagram correlating primary and secondary paleoseismic evidence to earthquake magnitude. (Modified from McCalpin [6])

The use of primary evidence for assessing the seismic hazard in the CEUS is limited because the thick overburden has precluded the manifestation of surficial features, and it is likely that many strong earthquakes produced no near-surface faults or associated deformations. Additionally, primary evidence does not provide any information regarding the areal distribution of the strength of shaking. This shortcoming is particularly important for the CEUS because of the limited historical data regarding the attenuation of seismic waves from the earthquake source. In contrast, secondary evidence, such as paleoliquefaction features, provides direct evidence of the areal distribution of the strength of shaking, even when the exact location of the seismogenic fault responsible for the secondary evidence is unknown (McCalpin [6]). Three areas of relatively high seismicity in the CEUS where paleoliquefaction investigations have been used to help assess seismic hazard are shown in Figure 5. These include the coastal region of South Carolina (e.g., Weems [11]; Amick [12]; Talwani [13]), the Wabash Valley Seismic Zone of southern Indiana/Illinois (e.g., Munson [9]; Pond [14]; Munson [15]; Hajic [16]; Obermeier [17]), and the New Madrid Seismic Zone (Tuttle [10]). All three of these areas in the CEUS share common uncertainties in geologic aspects of interpretation, in that some liquefaction effects have not been attributed to specific paleoearthquakes (i.e., exact dating of features has not be possible in some cases). This geologic uncertainty causes major questions regarding the level of prehistoric strength of shaking in these cases.

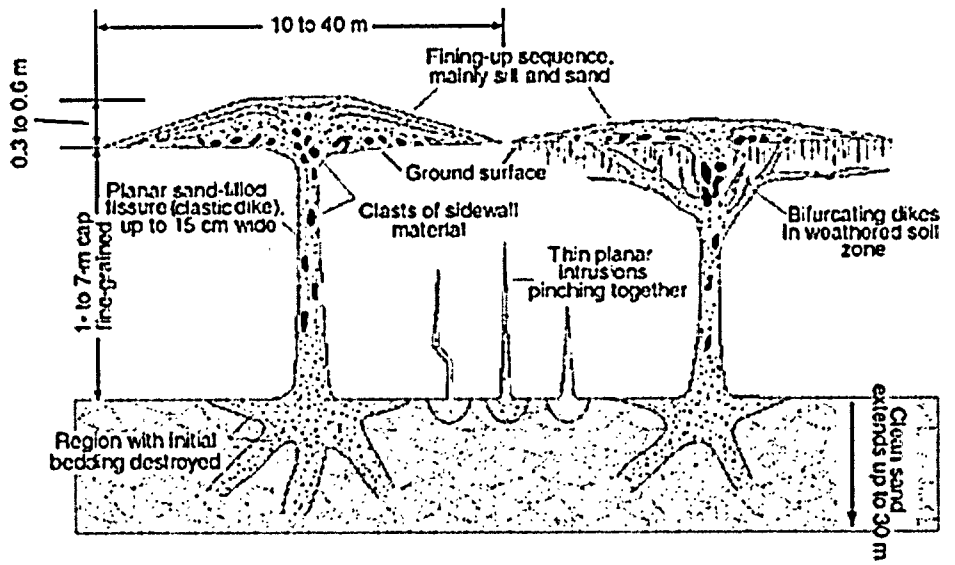

Figure 4. Schematic cross sectional view of sand boil, which is evidence of the occurrence of liquefaction. (From Obermeier [18])

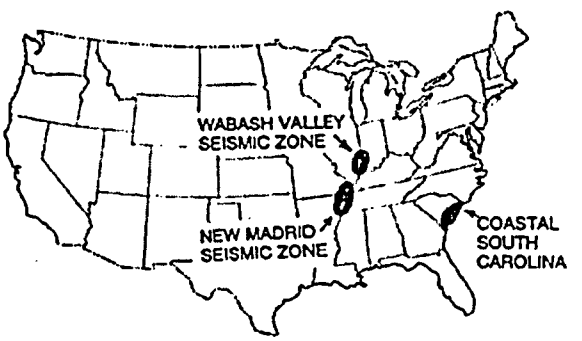

Figure 5. Locations of three seismically active regions of the CEUS where paleoliquefaction investigations have been used to assess seismic hazard. (From Obermeier [18])

ESTIMATION OF EARTHQUAKE STRENGTH OF SHAKING FROM PALEOLIQUEFACTION FEATURES

In a series of recent papers (Obermeier [1], Olson [2], and Green [3]), the authors describe in detail procedures and approaches to answer the three fundamental questions that provide the impetus for all paleoliquefaction investigations:

1. Has there been strong Holocene/late Pleistocene shaking in the area?
2. Where was the tectonic source?
3. What was the strength of strength of shaking?

In the following sections, the main components of the approach proposed by the authors to address the third question are summarized, including the collection, the interpretation, and the geotechnical back-analysis of paleoliquefaction field data.

Collection and Interpretation of Field Data

Collection of geotechnical data for paleoliquefaction studies should focus on sites of marginal liquefaction where a sectional view of the feature(s) is available, as well as on the evaluation of the possible effects of aging on liquefaction susceptibility at the sites that experienced marginal liquefaction (Olson [2]). Because the geotechnical properties that have been collected at sites of historical liquefaction to develop liquefaction resistance relationships (such as the cyclic stress curve: Youd [19]) were all collected *after* the causative earthquake (Youd [20]; Olson [21]), potential changes in relative density resulting from post-earthquake reconsolidation do not need to be accounted for in back-analyses. That is, although it is the soil properties exhibited prior to the earthquake that actually control the triggering of liquefaction, back-analysis using analytical geotechnical procedures (such as the cyclic stress method) should be based on soil properties that would be exhibited shortly after the earthquake (i.e., a few months) in order to be consistent with the databases used to develop the empirical liquefaction resistance relationships. Furthermore, our recommendation to use sites of marginal liquefaction preferentially over sites of severe liquefaction should minimize potential changes in relative density related to liquefaction.

Because in-situ testing inherently is conducted many years after a paleoearthquake, one should also assess the effects of aging on the in-situ test index (e.g., penetration resistance) that may have occurred following the paleoearthquake and occurrence of liquefaction (Olson [22]; Olson [2]). One good method to assess the impact of aging is by performing in-situ tests at side-by-side sites of marginal liquefaction and no liquefaction, in field locales where the sediments at the adjacent sites are nearly the same in terms of depositional environment and age, and where there is a large difference in the age of the liquefaction feature and the age of the source sediment that liquefied. In this case, the large difference in ages should amplify any increases in penetration resistance caused by the aging. There are several combinations of conditions that can be used to assess the significance of post-liquefaction aging. Some of these combinations are illustrated in Figure 6 for sites where sectional view observations are available. Figure 6 clearly illustrates the multitude of factors that can impact the back-calculation of the strength of shaking. Olson [2] describe the flow charts in more detail and the authors note that by using their method of side-by-side testing, the maximum strength of paleoseismic shaking can always be determined. Other approaches are available to assess aging, as was done for evaluation of actual field sites of the Vincennes Earthquake of the Wabash Valley (Green [3]). There, the authors were able to show that the effects of aging was almost certainly relatively minor except for very loose to loose sands, for time periods extending through 5,000 or so years.

The ground failure mechanism and severity of liquefaction also must be considered in the back-analysis, particularly with respect to selecting a "representative" penetration resistance for the liquefiable source bed. Each of the three principal modes of failure (i.e., hydraulic fracturing, surface oscillations, and lateral spreading) require a different minimum lateral extent of liquefaction to form liquefaction features. For example, lateral spreading requires liquefaction over a larger areal extent than does hydraulic fracturing. Thus, the field testing program should be set up so as to determine appropriate penetration resistance values for the sites that liquefied.

Lastly, multiple penetration tests are required to substantiate the selection of the "representative" penetration resistance. Table 1 provides the authors' recommendations for selecting the "representative" penetration resistance considering the ground failure mechanism, the severity of liquefaction, and the method in which the feature(s) are observed (i.e., in cross-sectional view or in plan view). Additional discussion as well as examples are provided in Olson [2] and Green [3]. The authors note that use of our "representative" penetration resistance provides a reasonable estimate of the lower limit of regional paleoseismic strength of shaking, when used in conjunction with our procedure below for evaluation of the regional pattern of strength of shaking.

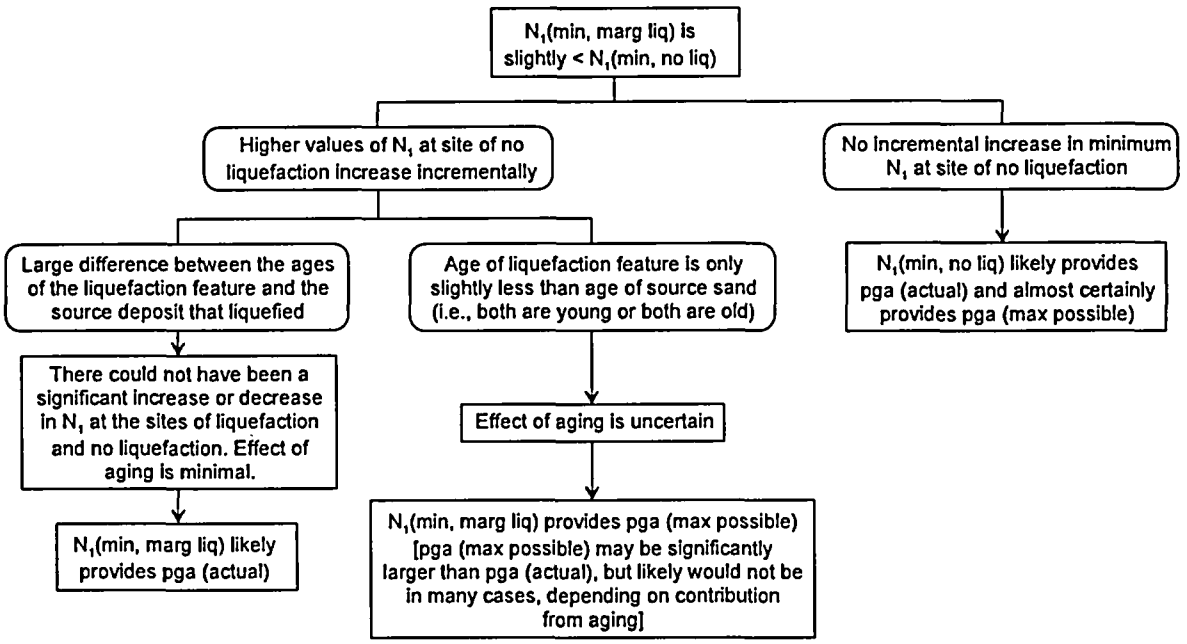

Figure 6a. Flow chart for back-calculation using marginal liquefaction features observed in sectional view where minimum SPT blowcount (corrected for energy ratio and overburden pressure) at marginal liquefaction site is only slightly less than minimum SPT blowcount at adjacent site of no liquefaction. (From Olson [2])

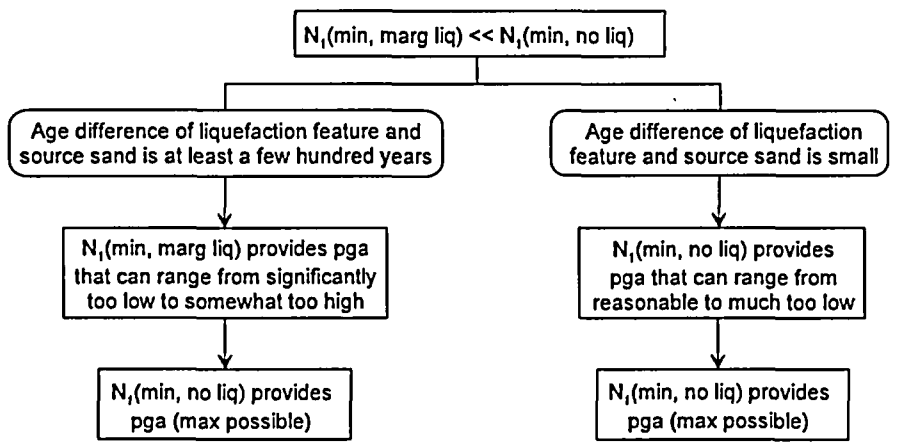

Figure 6b. Flow chart for back-calculation using marginal liquefaction features observed in sectional view where minimum SPT blowcount (corrected for energy ratio and overburden pressure) at marginal liquefaction site is much less than minimum SPT blowcount at adjacent site of no liquefaction. (From Olson [2])

Table 1. Guidelines for Selecting a Representative Penetration Resistance Value. (From Olson [2]).

Ground Failure Mechanism	Sectional View Observations of Marginal Liquefaction	Plan View Observations (any severity of liquefaction) and Sectional View Observations of Severe Liquefaction
Hydraulic fracturing	Designate individual penetration tests as locations of marginal liquefaction or no liquefaction based on proximity to observed liquefaction features. Use lowest value of penetration resistance at each test location.	Use highest minimum value of penetration resistance that is common among multiple penetration tests performed in proximity to individual liquefaction features created by hydraulic fracturing.
Lateral spreading	Designate penetration tests within the probable limits of lateral spread as marginal liquefaction. Designate tests outside these limits as no liquefaction. Use highest minimum value of penetration resistance common among multiple tests for each designation.	Use highest minimum value of penetration resistance that is common among penetration tests scattered along the length of the lateral spread (regardless of their proximity to venting features). This length can be hundreds of meters at places subjected to strong earthquake shaking.
Surface oscillations	Same as for hydraulic fracturing. Penetration tests should be performed within a few meters of observed liquefaction feature.	Use highest minimum value of penetration resistance that is commonly present (and typically near the base of the fine grained cap), and is located within a few tens of meters of the dikes caused by surface oscillations.
Indeterminate mechanism	Same as for hydraulic fracturing	Use lowest value of penetration resistance that is realistically feasible for any of the three candidate mechanisms listed above.

Geotechnical Back-Analysis of Paleoliquefaction Data

Once the field study is complete and interpretations of ground failure mechanism and representative penetration resistance have been made, the strength of shaking can be estimated for individual sites of liquefaction, marginal liquefaction, or no liquefaction. For illustration purposes, the steps will be presented below with reference to a marginal liquefaction site using the cyclic stress method (e.g., Youd [19]), although the overall approach applies equally to most other liquefaction evaluation procedures. Also, in the discussion below, the in-situ index is quantified in terms of $N_{1,60}$; however, the approach is applicable to any in-situ indices for which liquefaction evaluation procedures have been developed (e.g., q_{T1}, V_{s1}).

Once a representative $N_{1,60}$ is determined for a site, all a_{max}-M combinations required to induce liquefaction can be determined by setting the factor of safety against liquefaction (FS_{liq}) equal to one:

$$FS_{liq} = \frac{CRR}{CSR_{M7.5}} = 1 \tag{1}$$

Thus by substituting expressions for CRR (cyclic resistance ratio) and $CSR_{M7.5}$ (cyclic stress ratio for a M7.5 earthquake) into Eq. (1), peak ground acceleration (a_{max}) can be expressed as a function of M:

$$a_{max} = CRR(N_{1,60}) \cdot MSF(M) \cdot K_{\sigma} \cdot \frac{g \cdot \sigma'_{vo}}{0.65 \cdot \sigma_{vo} \cdot r_d} \tag{2}$$

where MSF is a magnitude scaling factor, K_σ is an overburden correction factor, g is the acceleration of gravity, σ'_{vo} and σ_{vo} are the effective and total vertical stresses, respectively, and r_d is a depth reduction factor. All of these factors (except g) are defined by Youd [19]. Figure 7 shows a plot of Eq.(2).

As may be observed from Figure 7a, the possible a_{max}-M combinations sufficient to induce liquefaction are wide ranging. Regional attenuation relations, in conjunction with the distance from the paleoliquefaction site to the energy center of the earthquake, can be used to define, in a deterministic sense, credible a_{max}-M combinations, as illustrated in Figure 7b. The intersection of the boundary separating the zones of a_{max}-M combinations that are sufficient and insufficient to induce liquefaction and the curve defining credible a_{max}-M combinations is the lower bound of the a_{max}-M combination operative at a liquefaction of marginal liquefaction site. As illustrated in Figure 6, in some cases, this combination may provide a reasonable estimate of the actual a_{max} operative at sites of marginal liquefaction.

In many regions of the US and the world, attenuation relations do not exist for all site conditions, as is the case at present in the CEUS where the attenuation relations are primarily for rock sites. A variety of approaches of varying degrees of sophistication can be used to relate the a_{max} for rock determined from attenuation relations to the corresponding value for the site condition of interest, as discussed in Green [3].

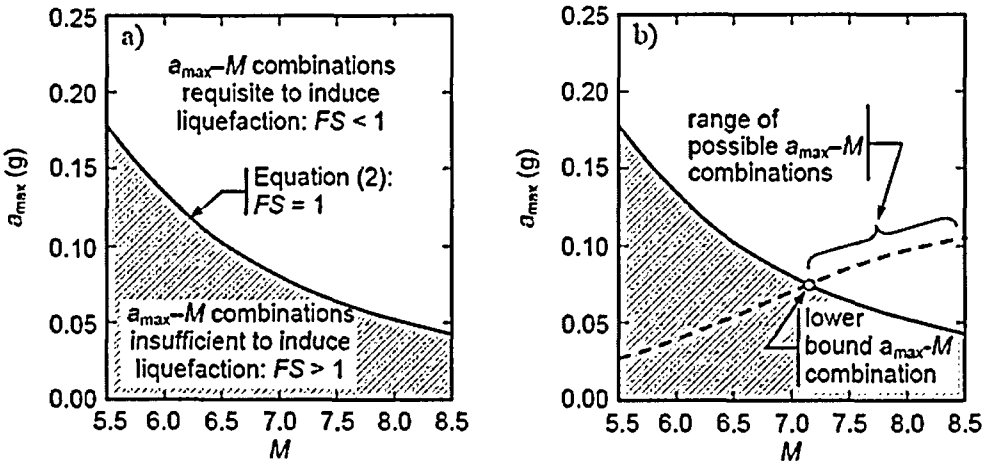

Figure 7. a) a_{max}-M combinations requisite to induce liquefaction. b) Determination of lower bound a_{max}-M combination using regional median a_{max} attenuation relation.

The above procedure was used to re-evaluate twelve paleoliquefaction sites in the Wabash Valley region of southern Indiana/Illinois (Figure 8), with the field data used in the evaluations coming from Pond [14]. The paleoliquefaction features are attributed to the Vincennes earthquake, which occurred approximately 6,100 years BP. The stress-based liquefaction evaluation procedure (e.g., Youd [19]) with magnitude scaling factors proposed by Andrus [23], in conjunction with the Somerville [24] attenuation relation and NEHRP [4] site response coefficients, were used to calculated the minimum a_{max}-M_w combinations required to induce liquefaction at each site. Table 2 lists the results of the analyses. For two of the sites (YO and PL), two different critical depths were identified, each corresponding to a different mode of liquefaction (e.g., hydraulic fracture and lateral spreading). Although not shown herein, similar calculations were performed by using other regionally applicable attenuation relations (i.e., Atkinson [25]; Toro [26]; Campbell [27]). These calculations produced nearly identical results in the regional assessment described subsequently.

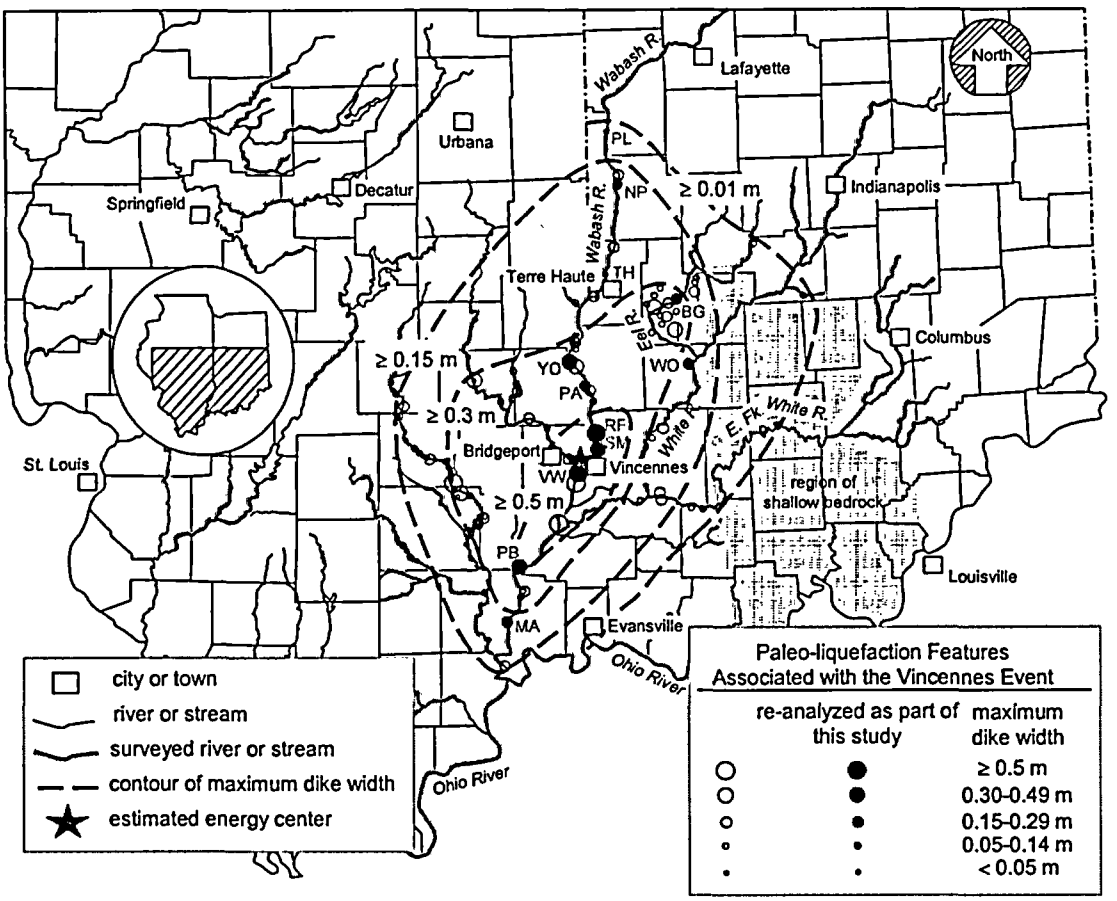

Figure 8. Map of southern Indiana/Illinois and the twelve paleoliquefaction sites analyzed in this study.

Following the approach outlined in Olson [2] and Green [3], the individual site a_{max}-M_w combinations were integrated in a regional assessment of the paleoearthquake magnitude. Several approaches can be used for the regional assessment, but the authors found the one illustrated in Figure 9 works well, particularly when uncertainty exists whether all the features analyzed were generated by the same causative earthquake. In Figure 9, three scenarios are shown. For each scenario the a_{max} values determined for each site are plotted as a function of the corresponding distances from the site to the hypothesized energy center of the earthquake, where the "+" and "-" signs indicate opposite directions from the energy center (e.g., North: + and South: -).

Scenario A in Figure 9 is for the case where all the paleoliquefaction features resulted from a single, large earthquake located at the hypothesized energy center. For such a scenario, it is likely that the data points for the sites will be symmetrical about a vertical line drawn through the location of the energy center (i.e., zero site-to-source distance). Using a regionally applicable a_{max} attenuation relation, and properly accounting for site amplification effects, the magnitude of the paleoearthquake is that corresponding to the contour of constant M that reasonably bounds the data points for the sites, as illustrated in the figure.

Table 2. Results from twelve fields sites of induced liquefaction in the Wabash Valley

Site	R_{hypo} (km)	Boring No.	Critical Depth (ft)		Depth gwt (ft)	N measured (bpf)	FC (%)	$N_{1,60cs}$ (bpf)	Earthquake Parameters	
			ATD	ATE					a_{max} (g)	M_w
VW	18	B-6	28	20	5	27	4	30.3	0.49	7.4
SM	25.1	B-2	12	7.75	0.75	7	4	8.9	0.16	6.2
RF	26.9	B-3	18.5	10.5	4	19	4	24.4	0.34	7.2
PA	37.4	B-2	20.5	8	7.5	12	4	13.6	0.26	7.2
PB	49	B-1	28	20	7.5	20	4	21.5	0.27	7.4
YO	60.8	B-2	28	16	10	12	4	12.1	0.19	7.3
		B-3	27	15.5	10.5	5	4	5.1	0.13	6.9
MA	79.6	B-3	10.5	7.5	4	9.5	10	13.2	0.17	7.5
WO	81.6	B-3	15	9	5	7	15	14.1	0.18	7.6
TH	93.5	B-1	34.5	17	2.5	14.5	4	16.8	0.15	7.6
BG	100.5	B-2	24	17.5	7.5	3.5	4	3.5	0.08	7.2
NP	135.4	B-1	23	10.5	6.5	6	4	7.1	0.10	7.8
PL	153.3	B-1	25.5	14	3	8	4	9.9	0.08	8.2
		B-2	30.5	18	2	4.5	4	5.1	0.06	7.9

Table notes:

- R_{hypo}: hypocentral distance to the paleoliquefaction sites
- Boring No.: boring number corresponding to the boring logs in Pond [14].
- Critical Depth: critical depth to liquefaction: ATD - in reference to the ground surface at time of drilling; ATE - in reference to the estimated ground surface at time of earthquake per Pond [14].
- Depth gwt: depth to ground water table at time of earthquake, in reference to the estimated ground surface at time of earthquake per Pond [14].
- N measured: measured SPT N-values.
- FC: fines content estimated from description given in boring logs of Pond [14].
- $N_{1,60cs}$: all corrections applied to measured SPT N-values are per Youd [19].
- For site PL no site amplification was applied to the Somerville [24] attenuation relations due to shallow depth to bedrock.

An alternative to single, large earthquake scenario (i.e., Scenario A) is the case where the liquefaction features were generated by a large earthquake and other smaller earthquakes that occurred in the same general locale in the same general time frame as the large earthquake. For this case the difference in the ages of the features generated by the large and smaller earthquakes would not be discernable using radiocarbon or other geologic dating techniques. This case is illustrated as Scenario B in Figure 9, with the resulting plot of the data being very similar to that for Scenario A.

The final scenario (Scenario C) illustrated in Figure 9 is that where the liquefaction features were induced by several small earthquakes occurring in the same general region and at about the same time. As with Scenario B, the difference in the ages of the features generated by the various earthquakes would not be discernable using radiocarbon or other geologic dating techniques. In contrast to Scenarios A and B, it is unlikely that a contour of constant M can be drawn using a regional attenuation relation that reasonably bounds the data for the sites. Depending on spatial distribution of the earthquakes, it is doubtful that the upper bound of the data points will be symmetrical about a vertical line drawn through the location of the hypothesized energy center (hypothesized, assuming the features were primarily induced by a single, large earthquake). Also, the maximum a_{max} (i.e., the a_{max} at the hypothesized energy center) for Scenario C will lower than for Scenarios A and B (i.e., $H_2 < H_1$).

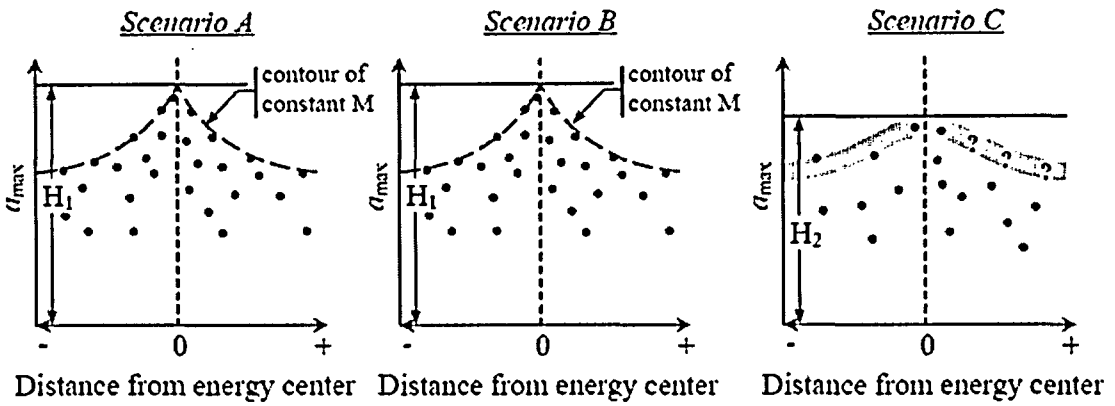

Figure 9. Illustration of potential scenarios that may occur when integrating the results from back-calculations of multiple paleoliquefaction sites in regionally assessing the magnitude of the paleoearthquake.

The above approach for integrating the data from the individual sites to regionally assess the magnitude of the Vincennes earthquake was applied to the data in Table 2, as shown in Figure 10. The open circles in this figure are for sites YO and PL, for which two potential critical depths to liquefaction were identified. The contours in Figure 10 were computed using the attenuation relation proposed by Somerville [24], with the NEHRP [4] site amplification factors applied. The assessment of the earthquake magnitude requires some judgment of the relative credibility of the calculated values for the individual sites. Based on the fact that some of the more northern sites in Figure 10 may be the result of liquefaction from an earthquake centered near there, and the fact that the authors have a high confidence in the representative penetration resistance values for all the sites south of Vincennes, interpretations based on the data for the three sites south of the epicenter are more credible than the northern sites. Consequently, the authors estimate that the magnitude of the Vincennes earthquake was approximately M7.5. The magnitudes for this event determined using three other regionally applicable attenuation relations (i.e., Atkinson [25]; Toro [26]; Campbell [27]) differed little from M7.5.

CONCLUSIONS

Similar to the assessment made for the Vincennes earthquake, assessments using the methods presented herein and detailed by Obermeier [1], Olson [2], and Green [3] could be made for other paleoliquefaction sites in the Wabash Valley, as well as sites in Charleston, South Carolina, in the New Madrid Seismic Zones, and in other tectonic settings worldwide. The assessed magnitude of the events using the proposed regional approach, in conjunction with the corresponding age of the induced features, allow the magnitude recurrence relations (Figure 2) to be established for a region, which in turn allows the seismic hazard of the region to be quantified probabilistically. The use of paleoliquefaction investigations for such a purpose removes the greatest impediment to implementing PBEE in the CEUS.

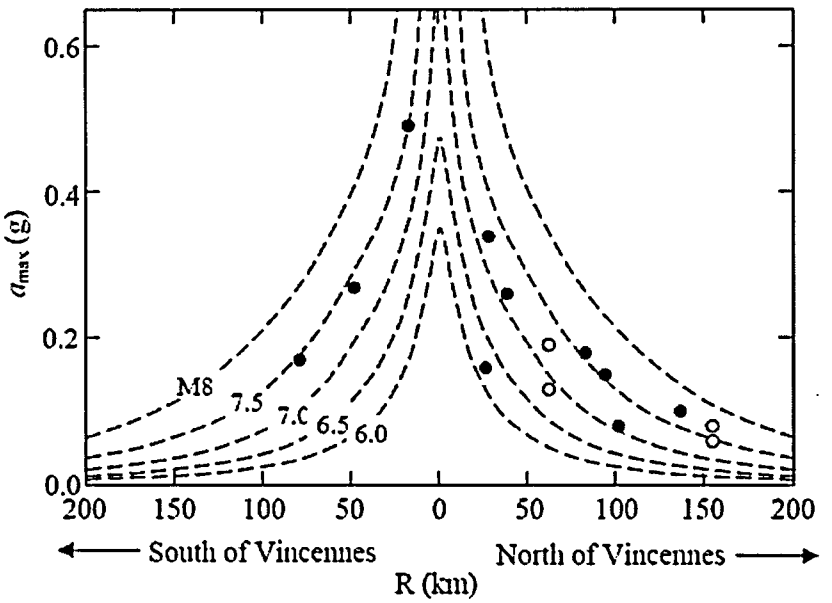

Figure 10. Regional assessment of the magnitude of the Vincennes earthquake. Open circles are for sites where multiple interpretations were made.

REFERENCES

1. Obermeier SF, Olson, SM, Green RA. "Field Occurrences of Liquefaction-Induced Features: A Primer for Engineering Geologic Analysis of Paleoseismic Shaking", Engineering Geology: An International Journal 2004, (in press).
2. Olson, SM, Green, RA, Obermeier, SF. "Engineering Geologic and Geotechnical Analysis of Paleoseismic Shaking Using Liquefaction Effects: A Major Updating", Engineering Geology: An International Journal 2004, (in press)
3. Green RA, Olson SM, Obermeier SF. "Engineering Geologic and Geotechnical Analysis of Paleoseismic Shaking Using Liquefaction Effects: Field Examples", Engineering Geology: An International Journal 2004, (in review).
4. NEHRP. "NEHRP Recommended Provisions for Seismic Regulations for New Buildings and Other Structures." Part 2 – Commentary, FEMA 369, Federal Emergency Management Agency, Washington, DC, 2001.
5. Schwartz DP, Coppersmith KJ. "Fault behavior and characteristic earthquakes: examples from the Wasatch and San Andreas faults." Journal of Geophysical Research 1984; 89: 5681-5698.
6. McCaplin JP, Nelson AR. "Introduction to Paleoseismology." Chapter 1, Paleoseismology (J.P McCaplin, ed.), Academic Press, New York, NY, 1996.
7. Wells, DL, Coppersmith, KJ. "Empirical Relationships Among Magnitude, Rupture Length, Rupture Area, and Surface Displacement." Bulletin of the Seismological Society of America 1994, 84(4):974-1002.
8. Ambraseys, NN. "Engineeing Seismology." Earthquake Engineering and Structural Dynamics 1988, 17: 1-105.
9. Munson, PJ, Munson, CA. "Paleoliquefaction evidence for recurrent strong earthquakes since 20,000 yr BP in the Wabash Valley of Indiana: Final report." submitted to the US Geological Survey, March, 1996, 137 p.

10. Tuttle, MP, Schweig, ES, Sims, JD, Lafferty, RH, Wolf, LW, Haynes, ML. "The Earthquake Potential of the New Madrid Seismic Zone." Bulletin of the Seismological Society of America 2002, 92(6): 2080-2089.
11. Weems, RE, Obermeier, SF. "The 1886 Charleston Earthquake – An Overview of Geologic Studies." Proc. 17th Water Reactor Safety Information Meeting, Report NUREG/CP-0105, US Nuclear Regulatory Commission 1990: 289-313.
12. Amick, D, Gelinas, R. "The Search for Evidence of Large Prehistoric Earthquakes along the Atlantic Seaboard." Science 1991, 251: 655-658.
13. Talwani, P, Schaeffer, WT. "Recurrence rates of large earthquakes in the South Carolina Coastal Plain based on paleoliquefaction data." J. of Geophysical Research 2001, 106(B4): 6621-6642.
14. Pond, EC, Martin, JR. "Seismic parameters for the central United States based on paleoliquefaction evidence in the Wabash Valley." Final Report Submitted to the USGS, August 1996, 583 p.
15. Munson, PJ, Obermeier, SF, Munson, CA, Hajic, MR. "Liquefaction evidence for Holocene and latest Pleistocene seismicity in the southern halves of Indiana and Illinois - a preliminary overview." Seismological Research Letters 1997, 68(4): 521-536.
16. Hajic, ER, Wiant, MD. "Dating of prehistoric earthquake liquefaction in southeastern and central Illinois: Final Report." submitted to the US Geological Survey, November, 1997, 57 p.
17. Obermeier, SF. "Liquefaction evidence for strong earthquakes of Holocene and latest Pleistocene ages in the states of Indiana and Illinois, USA." Engineering Geology 1998, 50: 227-254.
18. Obermeier SF. "Seismic Liquefaction Features: Examples from Paleoseismic Investigations in the Continental United States." U.S. Geological Survey Open-file Report 98-488, 1999.
19. Youd, TL, Idriss, IM, Andrus, RD, Arango, I, Castro, G, Christian, JT, Dobry, R, Finn, WDL, Harder, LF, Hynes, ME, Ishihara, K, Koester, JP, Liao, SSC, Marcuson, WF, Martin, GR, Mitchell, JK, Moriwaki, Y, Power, MS, Robertson, PK, Seed, RB, Stokoe, KH. "Liquefaction Resistance of Soils: Summary Report from the 1996 NCEER and 1998 NCEER/NSF Workshops on Evaluation of Liquefaction Resistance of Soils." Journal of Geotechnical and Geoenvironmental Engineering 2001, 127(10): 817-833.
20. Youd, TL. written communication with SF Obermeier 1999.
21. Olson, SM, Stark TD. "CPT based liquefaction resistance of sandy soils." Geotechnical Earthquake Engineering and Soil Dynamics III, ASCE Geotechnical Special Publication No. 75, 1: 325-336.
22. Olson, SM, Obermeier, SF, Stark, TD. "Interpretation of Penetration Resistance for Back-analysis at Sites of Previous Liquefaction." Seismological Research Letters 2001, 72(1): 46-59.
23. Andrus, RD, Stokoe, KH. "Liquefaction Resistance Based on Shear Wave Velocity." Proc. of the NCEER Workshop on Evaluation of Liquefaction Resistance of Soils (T.L. Youd and I.M. Idriss, eds), Technical Report NCEER-97-0022, 1997, 89-128.
24. Somerville, P, Collins, N Abrahamson, N Graves, R, Saikia, C. "Ground Motion Attenuation Relations for the Central and Eastern United States, Final Report submitted to the US Geological Survey, 2001.
25. Atkinson, GM, Boore, DM. "Some Comparisons between Recent Ground Motion Relations." Seismologic Research Letters 1997, 68(1): 24-40.
26. Toro, GR, Abrahamson, NA, Schneider, JF. "Model of Strong Ground Motions from Earthquakes in Central and Eastern North America: Best Estimates and Uncertainties." Seismologic Research Letters 1997, 68(1): 41-57.
27. Campbell, KW. "Development of Semi-Empirical Attenuation Relationships for the CEUS." USGS Annual Technical Summary 2001.